The Gas Phase Ion Chemistry of BH_2^+

Charles H. DePuy,*,† Roustam Gareyev,† Joseph Hankin,† Gustavo E. Davico,† Michèle Krempp,‡ and Robert Damrauer*,‡

Contribution from the Department of Chemistry and Biochemistry, University of Colorado at Boulder, Boulder, Colorado, 80309-0215, and Department of Chemistry, University of Colorado at Denver, Denver, Colorado, 80217-3364

Received November 24, 1997

Abstract: The reactions of BH_2^+ with hydrogen and some simple hydrocarbons and hydrides have been studied in the gas phase with a tandem flowing afterglow-selected ion flow tube apparatus. Reaction rate constants are reported along with branching ratios for multichannel reactions. The mechanisms of reactions have been elucidated by using deuterium labeling experiments and post-SCF level molecular orbital calculations. A general mechanism for the reaction $BH_2^+ + RH \rightarrow HBR^+ + H_2$ (R = OH, NH_2, SH, CH_3, C_2H_5, C_2H_3, C_2H) is suggested along with alternative and secondary pathways. Predicted intermediates have been generated by independent approaches. The unusual species BH_4^+ and BH_6^+ have been generated and their structures assessed computationally. The role of BH_4^+ in the isotope exchange reaction of BH_2^+ with D_2 is discussed in detail. Parallels are drawn between reactions of BH_2^+ and CH_3^+ in the gas phase and differences are revealed and discussed.

Introduction

In the gas phase it is often relatively easy to generate and examine the chemistry of ionic species which are unknown in solution. In this paper we describe some of the chemistry of BH_2^+, an extremely interesting electrophilic species which undergoes many of the same types of reactions as CH_3^+, but with greater selectivity so that more details of its reaction mechanisms can be uncovered.

Our interest in borohydride cations was aroused by our observation of the host of borohydride anions[1] which are produced upon ionization of B_2H_6 in our flowing afterglow-selected ion flow tube (FA-SIFT) instrument, and our subsequent finding that a similarly large number of cations is produced under the same ionization conditions.[2] Dunbar was the first to note that a myriad of $B_nH_m^+$ ions are produced upon ionization of B_2H_6 in an ICR instrument,[3] and he was able to show that many of these species were produced by reactions of initially produced borohydride cations with diborane, but he did not investigate reactions of any specific ionic species. The ion chemistry of dialkyl and dialkoxy boron cations is being extensively studied in an ion cyclotron resonance instrument by Kenttämaa et al.,[4] but except for a few studies of B^+,[5] nothing is known about the chemical behavior of the simplest boron cations.

Experimental Section

The flowing afterglow-selected ion flow tube (FA-SIFT) instrument and practical details of typical experiments have been described in detail elsewhere.[6] Diborane was used as a 5% mixture with helium (Matheson). Other reagents were obtained commercially and used without further purification. Measured reaction rate constants are reproducible within ±10% or better. We estimate the absolute error as ±20%. Branching ratio measurements (for reactions yielding more than one product) were corrected to account for mass discrimination of the quadrupole detection unit.

Calculations were performed with Gaussian 94[7] and Spartan v.4.0[8] software packages on IBM RS-6000 and SGI Indigo[2] computers, respectively.

Results and Discussion

The spectrum of B_2H_6 obtained under low-pressure conditions in a conventional mass spectrometer is dominated by the $B_2H_5^+$ ion (parent ion signal is negligible), accompanied by smaller peaks corresponding to its fragmentation. In contrast, in the FA-SIFT instrument where B_2H_6 undergoes electron impact ionization in a moderate pressure of flowing helium (0.1−1 mTorr of B_2H_6 in 200−500 mTorr of He), a spectrum shown in Figure 1 is typically obtained with many peaks corresponding to mass/charge ratios (m/z) exceeding that of the parent ion.

(1) Krempp, M.; Damrauer, R.; DePuy, C. H.; Keheyan, Y. *J. Am. Chem. Soc.* **1994**, *116*, 3629−3630.

(2) DePuy, C. H.; Gareyev, R.; Hankin, J.; Davico, G. E.; Damrauer, R. *J. Am. Chem. Soc.* **1997**, *119*, 427−428.

(3) Dunbar, R. C. *J. Am. Chem. Soc.* **1968**, *90*, 5676−5682.

(4) (a) Ranatunga, T. D.; Kenttämaa, H. I. *J. Am. Chem. Soc.* **1992**, *114*, 8600−8604. (b) Ranatunga, T. D.; Kenttämaa, H. I. *Inorg. Chem.* **1995**, *34*, 18−27.

(5) (a) Schneider, F.; Zülicke, L.; Polàk, R.; Vojtík, J. *Chem. Phys. Lett.* **1984**, *105*, 608−611. (b) Sondergaard, N. A.; Sauers, I.; Jones, A. C.; Kaufman, J. J.; Koski, W. S. *J. Chem. Phys.* **1979**, *71*, 2229−2234. (c) Ottinger, C.; Reichmuth, J. *J. Chem. Phys.* **1981**, *74*, 928−933. (d) Kemper, P. R.; Bushnell, J. E.; Weis, P.; Bowers, M. T. *J. Am. Chem. Soc.* Submitted for publication.

(6) (a) Van Doren, J. M.; Barlow, S. E.; DePuy, C. H.; Bierbaum, V. M. *Int. J. Mass Spectrom. Ion Processes* **1987**, *81*, 85−100. (b) Gronert, S.; O'Hair, R. A. J.; Prodnuk, S.; Sülzle, D.; Damrauer, R.; DePuy, C. H. *J. Am. Chem. Soc.* **1990**, *112*, 997−1003. (c) Robinson, M. S.; Polak, M. L.; Bierbaum, V. M.; DePuy, C. H.; Lineberger, W. C. *J. Am. Chem. Soc.* **1995**, *117*, 6766−6778.

(7) Frisch, M. J.; Trucks, G. W.; Schlegel, H. B.; Gill, P. M. W.; Johnson, B. G.; Robb, M. A.; Cheeseman, J. R.; Keith, T.; Petersson, G. A.; Montgomery, G. A.; Raghavachari, K.; Al-Laham, M. A.; Zakrzewski, V. G.; Ortiz, J. V.; Foresman, J. B.; Cioslowski, J.; Stefanov, B. B.; Nanayakkara, A.; Challacombe, M.; Peng, C. Y.; Ayala, P. Y.; Chen, W.; Wong, M. W.; Andres, J. L.; Replogle, E. S.; Gomperts, R.; Martin, R. L.; Fox, D. J.; Binkley, J. S.; Defrees, D. J.; Baker, J.; Stewart, J. P.; Head-Gordon, M.; Gonzalez, C.; Pople J. A. *Gaussian 94, Revision C.2*; Gaussian, Inc.: Pittsburgh, PA, 1995.

(8) *Spartan version 4.0*; Wavefunction, Inc.

S0002-7863(97)04005-5 CCC: $15.00 © 1998 American Chemical Society
Published on Web 05/12/1998

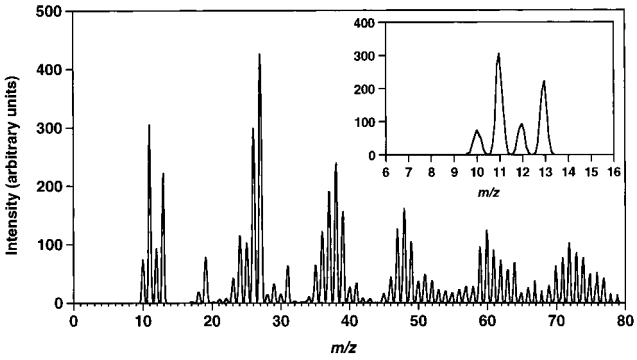

Figure 1. The electron impact ionization mass spectrum of diborane (0.3 mTorr) obtained under flowing afterglow conditions with a helium buffer gas pressure of 350 mTorr. The insert is the expanded view of the *m*/*z* 6−16 region of the spectrum.

This is indicative of secondary reactions of initially formed simple cations with diborane to form ions which incorporate more boron atoms. An important factor here is the interaction with the helium buffer gas which collisionally cools adducts and products of exothermic reactions which otherwise would dissociate back to simple particles. Therefore, one expects that the appearance of the resulting spectrum will depend on the amount of diborane added and the pressure of helium bath gas. Our studies show that higher flows of B_2H_6 and higher pressures of helium in the flow tube produce larger borohydride cluster cations at the expense of small ions. Since our goal is to study one of the smallest ions, we optimized the source conditions to produce large signals of BH_2^+ by using low diborane flows and moderate helium pressures.

Note that the peaks in Figure 1 fall into distinctive groups corresponding to ions that contain the same number of boron atoms but varying amounts of hydrogen. The spectrum is complicated further by the fact that naturally occurring boron consists of an 81:19 mixture of ^{11}B and ^{10}B isotopes, so that many of the peaks can be mixtures of isotopic but chemically different ions. Several peaks corresponding to products of reactions between traces of water and borohydride cations can also be identified (*vide infra*).

Let us examine more closely the region of the spectrum corresponding to ions containing one boron atom (the insert in Figure 1). The peak at *m*/*z* 10 should be a signal solely of $^{10}B^+$. The next peak, *m*/*z* 11, can correspond to $^{11}B^+$ and also to $^{10}BH^+$, while *m*/*z* 12 may be a mixture of $^{11}BH^+$ and $^{10}BH_2^+$. Finally, *m*/*z* 13 can, in principle, contain $^{11}BH_2^+$ and $^{10}BH_3^+$. However, if $^{10}BH_3^+$ were contributing to this peak, a peak at *m*/*z* 14 ($^{11}BH_3^+$) would necessarily be present since the ^{11}B:^{10}B ratio is 4:1. Since *m*/*z* 14 is not detected, the peak at *m*/*z* 13 must be the signal of $^{11}BH_2^+$ only. From a knowledge of the peak intensities at each *m*/*z* under discussion and the fact that *m*/*z* 10 and 13 are monoisotopic $^{10}B^+$ and $^{11}BH_2^+$, respectively, we can determine that *m*/*z* 11 is 97% $^{11}B^+$ and 3% $^{10}BH^+$, while *m*/*z* 12 is 39% $^{11}BH^+$ and 61% $^{10}BH_2^+$. The overall percentage of B^+, BH^+, and BH_2^+ produced is 53%, 6%, and 41%, respectively, under these conditions, with the ratio of ^{10}B and ^{11}B isotopomers being 1:4 for each ion.

One of the most important features of our FA-SIFT instrument is its capability of selecting reactant ions of a single *m*/*z* thus separating them from other constituents of a mixture. This allows injection of a pure population of $^{11}BH_2^+$ ions into the second (reaction) flow tube of the instrument, where their reactions with neutral reagents can be studied. This is illustrated in Figure 2 by a spectrum that shows the products of the reaction of $^{11}BH_2^+$ (*m*/*z* 13) with ethane added to the second flow tube:

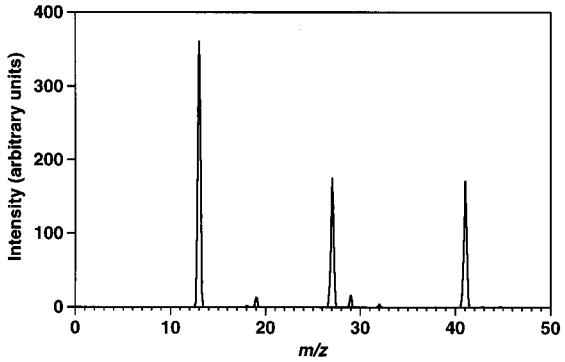

Figure 2. The experimental spectrum representing the reaction of $^{11}BH_2^+$ ion (*m*/*z* 13) with C_2H_6. Product ions are $C_2H_5BH^+$ (*m*/*z* 41) and CH_3BH^+ (*m*/*z* 27).

Table 1. Reactions of BH_2^+ in the Gas Phase

reagent	product(s) and branching ratio	secondary reaction	overall rate constant, $\times 10^{10}$ cm^3 $molecule^{-1}$ s^{-1} (efficiency)[b]
H_2 (M)[a]	BH_4^+	$BH_4^+ + H_2 \rightarrow BH_6^+$	N/A
D_2	BHD^+ (0.91)		0.36 (0.030)
	BD_2^+ (0.09)		
$BD_2^+ + H_2$	BHD^+ (0.93)		0.33 (0.021)
	BH_2^+ (0.07)		
H_2O	$HBOH^+$	$HBOH^+ + H_2O \rightarrow H_3O^+$	18.1 (0.70)
H_2S	$HBSH^+$	$HBSH^+ + H_2S \rightarrow H_3S^+$	16.0 (0.82)
NH_3	$HBNH_2^+$	$HBNH_2^+ + NH_3 \rightarrow NH_4^+$	20.9 (0.88)
CH_4	$HBCH_3^+$		9.07 (0.64)
C_2H_6	$HBC_2H_5^+$ (0.5)		13.4 (0.82)
	$HBCH_3^+$ (0.5)		
C_2H_4	$BH_2C_2H_4^+$ (0.15)		15.0 (0.93)
	$HBC_2H_3^+$ (0.85)		
C_2H_2	HBC_2H^+		16.2 (1.00)

[a] Three-body association in the presence of helium atoms. [b] Relative to Langevin collision rate constants[21] for nonpolar neutral reagents and theoretical ADO rate constants[22] for polar reagents.

$C_2H_5BH^+$ (*m*/*z* 41) and CH_3BH^+ (*m*/*z* 27). A summary of some reactions of BH_2^+ studied is given in Table 1, in which branching ratios for multiple channel reactions and reaction rate constants are also reported.

One important transformation of BH_2^+ that should be mentioned before we proceed with a discussion of its chemical reactions is its collision-induced dissociation (CID). This occurs when the ions are given additional electrokinetic acceleration before injection into the reaction flow tube, so that collisions with helium atoms deliver enough energy to break the ions apart. When injected at laboratory frame kinetic energies above 30 eV, BH_2^+ exclusively loses a molecule of H_2 yielding B^+. Observation of only $^{11}B^+$ upon CID of ions of *m*/*z* 13 is a direct confirmation of the isotopic purity of this peak, and in the discussion below we will refer to $^{11}BH_2^+$ ions as BH_2^+ for simplicity.

The reactions of BH_2^+ are strikingly analogous to those of CH_3^+. Reactions of CH_3^+ with H_2 and CH_4 have been extensively studied both experimentally[9,10] and computationally.[11] We have therefore carried out ab initio molecular orbital (MO) calculations on the reactions of BH_2^+ with these reagents for comparison purposes. The computational results are summarized in Table 2, which also includes some results of our

(9) (a) Smith, D.; Adams N. G.; Alge, E. *J. Chem. Phys.* **1982**, *77*, 1261−1268. (b) Heck, A. J. R.; de Koning, l. J.; Nibbering, N. M. M. *J. Am. Soc. Mass Spectrom.* **1991**, *2*, 453−458. The results of the cited works discussed here were independently reproduced in our laboratory.

(10) Olah, G. A.; Prakash, G. K. S.; Williams, R. E.; Field, L. D.; Wade, K. *Hypercarbon Chemistry*; Wiley-Interscience: New York, 1987.

Table 2. Results of *Ab Initio* Molecular Orbital Calculations[a]

species[b]	symmetry	MP2(full)/6-311G(d,p)	N_{imag}[c]	ZPE[d]	QCISD(T)/CC-pVTZ	G2	CBS-Q
BH_2^+ (3a)	$D_{\infty h}$	−25.5526	0	0.0178	−25.5651	−25.5568	−25.5543
BH_4^+ (3b)	C_{2v}	−26.7406	0	0.0362	−26.7672	−26.7447	−26.7421
BH_4^+ (3c)	C_{2v}	−26.7121	1	0.0337		−26.7194	
BH_4^+ (3d)	C_{2v}	−26.7307	1	0.0336		−26.7384	
BH_6^+ (3e)	C_{2v}	−27.9351	0	0.0566	−27.9754	−27.9377	−27.9343
$CH_4BH_2^+$ (7a)	C_{2v}	−66.0065	0	0.0685			
$CH_3HBH_2^+$ (7b)	C_s	−65.9637	1	0.0636			
$CH_3BH(H_2)^+$ (7c)	C_1	−65.9953	0	0.0639			
CH_3BH^+ (7d)	C_{3v}	−64.8284	0	0.0459			
$CH_3CH_3BH_2^+$ (9a)	C_s	−105.2312	0	0.0985			
$CH_3HCH_2BH_2^+$ (9b)	C_1	−105.1936	1	0.0945			
$CH_4CH_2BH_2^+$ (9c)	C_1	−105.1949	0	0.0955			
$CH_4CH_2HBH^+$ (9d)	C_1	−105.1747	1	0.0905			

[a] Energies are in hartrees. [b] Expressions in parentheses refer to the figure number and the structure in that figure. [c] Number of imaginary vibrational frequencies. [d] Zero-point vibrational energy correction from MP2(full)/6-311G(d,p) frequencies, unscaled.[23]

Table 3. Comparison of Binding Energies (kcal mol^{-1}) of the First and the Second Hydrogen Molecules to BH_2^+ to Form BH_4^+ and BH_6^+, Respectively, Calculated at Different Levels of Theory

	$BH_2^+ + H_2 \rightarrow BH_4^+$	$BH_4^+ + H_2 \rightarrow BH_6^+$
MP2(full)/6-311G(d,p)	−12.3	−15.1
QCISD(T)/CC-pVTZ	−13.6	−16.2
G2	−13.5	−16.8
CBS-Q	−13.6	−16.4

highest level ab initio (QCISD(T)/CC-pVTZ) and model chemistry (CBS-Q,[12] G2[13]) calculations. Relevant molecular structures are presented in Figures 3, 7, and 9. Table 3 presents a comparison of computational results obtained at different levels of theory for binding energies of two molecules of hydrogen to BH_2^+ (see discussion below). The table shows that the MP2-(full)/6-311G(d,p)//MP2(full)/6-311G(d,p) level of theory adequately describes the energetics of this system, the discrepancy with computationally much more expensive methods being less than 2 kcal mol^{-1}. Therefore, results obtained at the MP2 level are used for discussion of geometries and energetics.

Reactions with D_2 and H_2. When BH_2^+ is allowed to react with D_2, moderately fast hydrogen−deuterium exchange occurs to form BHD^+ and BD_2^+ (Table 1). The branching ratio for these two products is dependent on reaction time, and the value of 0.91:0.09 BHD^+/BD_2^+ was determined by extrapolating the experimental data to zero reaction time. In a mirror experiment $^{11}BD_2^+$ was generated in the source flow tube by adding D_2 to the flow of B_2H_6 being ionized. This ion (*m*/*z* 15) was then mass selected and injected into the reaction flow tube to study its isotope exchange reaction with H_2. As Table 1 shows, the reverse reaction is slightly slower and the amount of double exchange is correspondingly smaller than for the reaction of BH_2^+ with D_2, indicating a primary kinetic isotope effect.

We have investigated this exchange reaction by *ab initio* MO calculations, and the elucidated mechanism is presented in Figure 4. Reaction of BH_2^+ (**I**) with D_2 first leads to a planar adduct (**II**) (structure **b** in Figure 3). In a majority of encounters this intermediate dissociates back to reactants, but occasionally it isomerizes through transition state **III** (structure **c** in Figure 3) into **IV**. This complex most commonly dissociates to give the primary product of reaction **V**, but may in some instances undergo another isomerization to **VI**, giving rise to some amount of the doubly exchanged product **VII**.

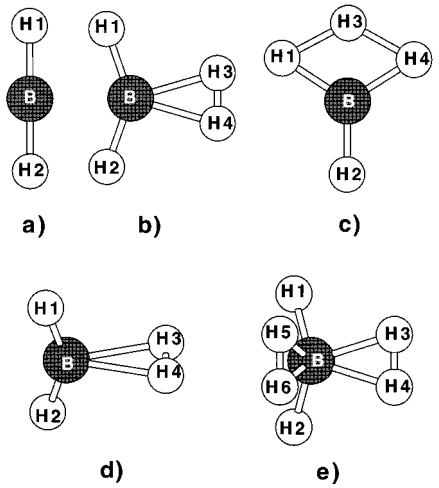

Figure 3. Molecular structures of BH_2^+ (a), BH_4^+ (b), BH_6^+ (e), and two transition states of BH_4^+ (c, d) optimized at the MP2(full)/6-311G-(d,p) level of theory.

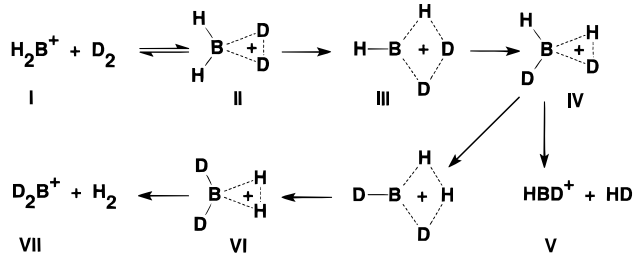

Figure 4. Proposed mechanism for isotope exchange in the reaction of BH_2^+ with D_2.

The energy profile of this process for the symmetric reaction of BH_2^+ with H_2 is shown in Figure 5. The initial $H_2BH_2^+$ adduct is more stable than the reactants by about 13 kcal mol^{-1} (Table 3), while the transition state for isomerization lies slightly above the entrance channel. Consequently, most of the initially formed complex does not have sufficient energy to surmount the barrier, and dissociates back, causing the low efficiency of the exchange reaction. For those molecules that cross the barrier, dissociation is more favorable than further isomerization, so that the majority of product ions formed in a single reactive encounter have undergone exchange of only one hydrogen.

(11) (a) Schleyer, P. v. R.; Carneiro, J. W. d. M. *J. Comput. Chem.* **1992**, *13*, 997−1003. (b) Schreiner, P. R.; Kim, S.-J.; Schleyer, P. v. R.; Schaefer, H. F., III *J. Chem. Phys.* **1993**, *99*, 3716−3720. The results of the cited works were reproduced by using the uniform MP2(full)/6-311G(d, p)//MP2-(full)/6-311G(d, p) method for comparison purposes.

(12) Ochterski, J. W.; Petersson, G. A.; Montgomery, J. A., Jr. *J. Chem. Phys.* **1996**, *104*, 2598−2619.

(13) Curtiss, L. A.; Raghavachari, K.; Trucks, G. W.; Pople, J. A. *J. Chem. Phys.* **1991**, *94*, 7221−7230.

(14) For a preliminary account of the results discussed in this section see ref 2.

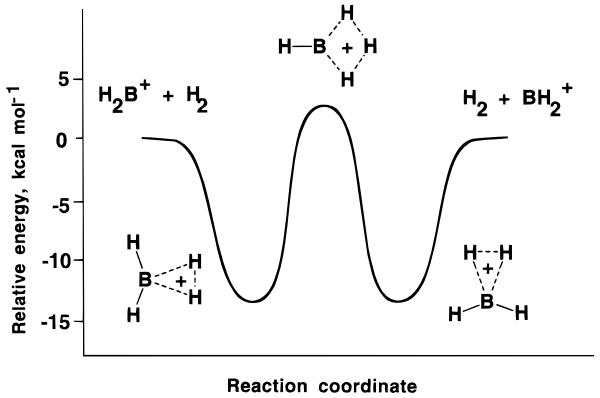

Figure 5. The calculated potential energy profile for the symmetric reaction of hydrogen exchange in BH_2^+.

The lowest energy structure of the adduct BH_4^+ is planar (structure **b** in Figure 3), with BH_2^+ forming a three-center two-electron bond with the hydrogen molecule. As might be expected from the rather weak bond (12.3 kcal mol^{-1}, Table 3), the B−H3 bond is quite long (1.446 Å, compared to 1.175 Å for B−H1 and 1.173 Å in BH_2^+), and the H3−H4 distance (0.808 Å) is only slightly lengthened from its normal distance in H_2 of 0.738 Å. Square planar (D_{4h}) and tetrahedral (T_d) structures for BH_4^+ are higher in energy by about 30 and 170 kcal mol^{-1}, respectively, and do not represent minima on the potential energy surface. Somewhat surprisingly from a steric point of view, an adduct with the H_2 molecule twisted orthogonal to the H1−B−H2 plane (structure **d** in Figure 3) is *less* stable than the planar adduct by 4.6 kcal mol^{-1} and represents a transition state structure for rotation of the H_2 molecule with respect to the symmetry axis of the adduct.

These computational results and experimental data discussed above are in striking contrast with those for reaction of CH_3^+ with H_2 (D_2), which has been extensively studied previously. Methyl cation forms an adduct with H_2 that is bound by 42 kcal mol^{-1} [11] and CH_5^+ ion can be observed experimentally in the gas phase[9] or in superacid media.[10] Reaction with D_2 leads to fast isotope exchange with complete scrambling of all hydrogen and deuterium atoms within the reaction complex of CH_3^+ with D_2. The calculated central barrier for this process is less than 1 kcal mol^{-1} [11] (compared to 16 kcal mol^{-1} for BH_2^+). Calculations show that in $CH_3-H_2^+$ the distance from the carbon atom to the added hydrogen atoms is 1.197 Å, just slightly longer than the distance to the native hydrogens (1.093 Å), and the H−H bond is significantly stretched (0.930 Å). There is virtually no barrier to rotation of the H_2 moiety relative to the CH_3^+ group in this adduct. Most of these differences are easily explained in terms of the lower electrophilicity of BH_2^+ and hence a weaker binding interaction and a less pronounced reactivity. However, the unexpected stability of the planar BH_4^+ adduct compared to its orthogonal conformer and the considerable barrier to rotation of the H_2 moiety in it (4.6 kcal mol^{-1}) require additional scrutiny.

Examination of the molecular orbitals of BH_4^+ reveals that in addition to direct bonding by interaction of the σ-bonding molecular orbital of H_2 with the vacant π-orbital of the boron atom (formation of a 3-center 2-electron bond) there is considerable overlap of the antibonding σ^* MO of H_2 with the lower lying occupied MO of BH_2^+. This interaction leads to a highest occupied MO of BH_4^+ with the shape presented in Figure 6a. In this HOMO BH_2^+ is effectively donating some of its electron density to the vacant MO of H_2. This stabilizing interaction is back-bonding, in the sense that the electron shift occurs in the direction opposite to normal bonding where the electrophilic boron withdraws electronic density from the occupied σ MO of the dihydrogen molecule. This back-bonding accounts for approximately one-third of the total binding energy of H_2 to BH_2^+ (4.6 out of 12.3 kcal mol^{-1}). The overlap and additional bonding do not occur in the conformation of BH_4^+ with H_2 perpendicular to the plane of BH_2^+ (Figure 6b).

Experimental Observation of BH_4^+ and BH_6^+.[14] Although the formation of BH_4^+ is implicated by the isotope exchange reaction of BH_2^+ with D_2 and predicted computationally, no $BH_2D_2^+$ (or BH_4^+) was observed under typical conditions in our instrument (helium buffer gas pressure of 0.5 Torr, neutral reagent densities on the order of 10^{11} particles cm^{-3}). In an attempt to facilitate adduct formation we increased the helium pressure in the reaction flow tube to 0.75 Torr (to enhance collisional cooling of the product of this three-body association reaction) and the H_2 density to over 10^{15} particles cm^{-3} (to shift the equilibrium of the reaction toward the complex). Indeed, a peak at *m*/*z* 15, as expected for BH_4^+, appeared in the spectrum. More surprisingly, a noticeable peak appeared at *m*/*z* 17, which corresponds to BH_6^+, an adduct of BH_2^+ with two molecules of hydrogen. At sufficiently high concentrations of hydrogen the intensity of this peak was even larger than that for *m*/*z* 15.

Although no other positive ions can occur at *m*/*z* 17 under the experimental conditions employed (OH^+ or NH_2^+ which might be produced from traces of air or water are unstable and would readily react with the huge amounts of H_2 present), we undertook thorough experiments to prove the formation of the BH_6^+ adduct. No ionic products with *m*/*z* 17 (and *m*/*z* 15 as well) were observed when BH_2^+ was allowed to react with H_2O, NH_3, or CH_4 (Table 1), which are each conceivable sources of other ions with the same mass-to-charge ratio. Mass-selected injection of isotopically labeled $^{10}BH_2^+$ (*m*/*z* 12) and its reaction with dihydrogen leads to the formation of the corresponding ions of *m*/*z* 14 ($^{10}BH_4^+$) and *m*/*z* 16 ($^{10}BH_6^+$). Another indicator of the formation of BH_6^+ is the reaction of BH_2^+ with D_2 under the same conditions to give ions of *m*/*z* 23 ($^{11}BD_6^+$), which result from complete H−D exchange in BH_2^+ and consequent complexation of two D_2 molecules.

The structure of BH_6^+ also has been investigated theoretically. By analogy with the structure of BH_4^+, in which one empty *p* orbital of BH_2^+ complexes with H_2, we assumed that in BH_6^+ both empty *p* orbitals are used in complexation to form a near-tetrahedral ion, with boron hybridized sp^3 and with the two H_2 molecules bonded by 3-center 2-electron bonds. Indeed, the optimized structure presented in Figure 3e was found to be an energy minimum. Surprisingly, the binding energy for the second hydrogen molecule (15.1 kcal mol^{-1}) is greater than that for the first one (12.3 kcal mol^{-1}) (Table 3). Bond lengths are also somewhat different than in BH_4^+, the B−H3 distance being considerably shorter (1.386 Å in BH_6^+ versus 1.446 Å in BH_4^+) and the H3−H4 distance increasing (0.818 Å in BH_6^+, as compared to 0.808 Å in BH_4^+), giving another indication that the second H_2 is held more tightly. Back-bonding from the BH_2^+ moiety into the antibonding σ^* orbitals of the H_2 molecules also plays a significant role in the stability of BH_6^+, as shown in Figure 6c, which depicts the HOMO of BH_6^+. Additional stabilization is also provided by the completion of the electronic octet around the boron atom as two more electrons are brought in by the second hydrogen molecule.

Shortly after the publication of our preliminary report on the experimental observation of BH_4^+ and BH_6^+ and calculations of their structures and energetics,[2] a theoretical study of these two and some other related boronium ions by Rasul and Olah

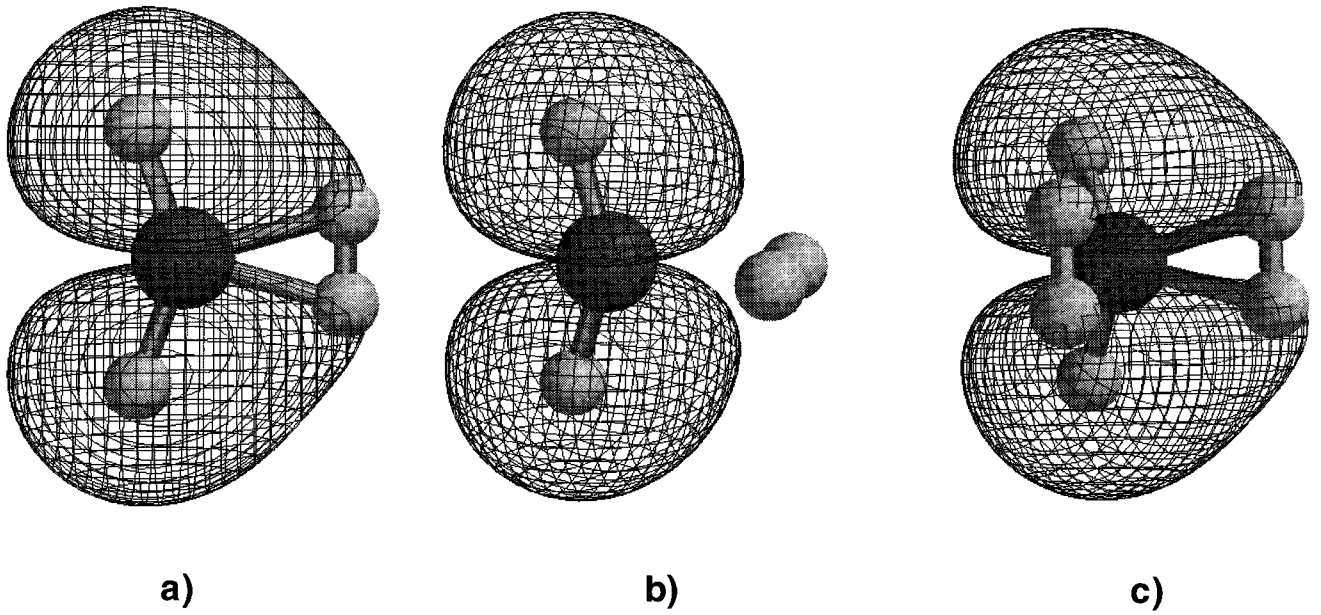

Figure 6. The highest occupied molecular orbitals of BH_4^+ (a, b) and BH_6^+ (c) as obtained by the Spartan program.

appeared,[15] predicting that these ions would be stable. Their calculations are in complete agreement with our own.

Although in this paper we show that the chemistry of BH_2^+ is remarkably similar to that of CH_3^+, BH_2^+ is isoelectronic with CH_2^{2+}, a species which is so far unknown experimentally. Theoretical investigations[16] showed that 3-center 2-electron bonding of a hydrogen molecule to CH_2^{2+} should lead to a minimum potential energy CH_4^{2+} species with a C_{2v} structure similar to that of BH_4^+. In related work, Olah, Schleyer, and co-workers[17] showed that a CH_6^{2+} species of C_{2v} symmetry also represents a minimum on the potential energy surface and has a structure close to that proposed above for BH_6^+.

Reaction with Methane. Methane reacts rapidly with BH_2^+ by addition and loss of a molecule of H_2 (Table 1), a reaction seemingly analogous to that of methane with CH_3^+:

$$CH_4 + CH_3^+ \rightarrow CH_3{-}CH_2^+ + H_2$$

However, when CH_3^+ reacts with CD_4, or CD_3^+ with CH_4, the proportion of H_2, HD, and D_2 being eliminated is close to random.[18] This indicates that near-complete scrambling of all hydrogen and deuterium atoms occurs before dissociation of an initially formed adduct. In contrast, reaction of BH_2^+ with CD_4, or BD_2^+ with CH_4, leads exclusively to loss of HD:

$$CD_4 + BH_2^+ \rightarrow CD_3{-}BH^+ + HD$$

$$CH_4 + BD_2^+ \rightarrow CH_3{-}BD^+ + HD$$

We investigated the origin of this surprising selectivity using theoretical calculations. The structures of key intermediates and transition states for the reaction of BH_2^+ with CH_4 are shown in Figure 7, and corresponding energies are listed in Table 2. Our calculations indicate the initial formation of a rather strongly bound (about 33 kcal mol^{-1}) adduct (structure **a** in Figure 7),

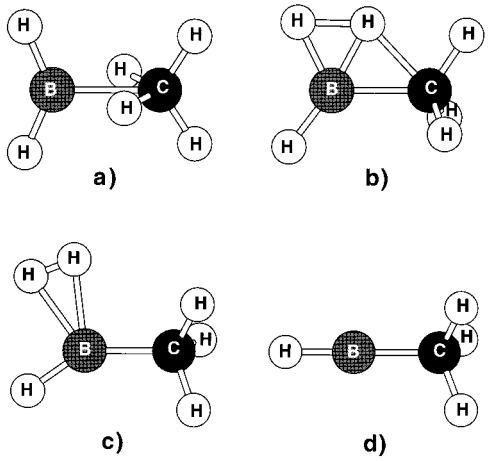

Figure 7. Molecular structures of species relevant to the reaction of BH_2^+ with CH_4 obtained from MP2(full)/6-311G(d,p) calculations.

followed by carbon−boron bond formation and hydrogen atom migration leading through transition structure **b** (Figure 7) to $CH_3BH(H_2)^+$ (**c** in Figure 7), a species homologous to BH_4^+. Because of the stabilizing effect of the methyl group on the adjacent positive charge, the hydrogen molecule in this cation is bound extremely weakly (<1 kcal mol^{-1}) and is eliminated readily giving the final product (**d** in Figure 7). (A similar effect of the methyl group can be found in comparison of CH_5^+ with $C_2H_7^+$—in the latter the hydrogen molecule is bound by only 10.6 kcal mol^{-1},[19] much weaker than in CH_5^+.) In the case of deuterium-labeled reagents this rapid dissociation leaves no possibility of hydrogen−deuterium scrambling and one atom of deuterium or hydrogen is lost from each of the heavy atoms, resulting in selective elimination of HD. Other conceivable reaction paths, such as elimination at the carbon atom leading to formation of carbocation $BH_2{-}CH_2^+$, prove to be endothermic and the corresponding structures do not represent minima on the potential energy surface.

The energy diagram for the reaction of BH_2^+ with CH_4 is shown in Figure 8. Note that the initial adduct lies in a relatively

(15) Rasul, G.; Olah, G. A. *Inorg. Chem.* **1997**, *36*, 1278−1281.
(16) Radom, L.; Wong, M. W. *J. Am. Chem. Soc.* **1989**, *111*, 1155−1166.
(17) Lammertsma, K.; Barzaghi, M.; Olah, G. A.; Pople, J. A.; Schleyer, P. v. R.; Simonetta, M. *J. Am. Chem. Soc.* **1983**, *105*, 5258−5263.
(18) (a) Weiner, J.; Smith, G. P. K.; Saunders: M.; Cross, R. J., Jr. *J. Am. Chem. Soc.* **1973**, *95*, 4115−4120. (b) Lee, H. S.; Bierbaum, V. M.; DePuy, C. H. *Int. J. Mass Spectrom. Ion Processes* In press.
(19) Carneiro, J. W. de M.; Schleyer, P. v. R.; Saunders, M.; Remington, R.; Schaefer, H. F., III; Rauk, A.; Sorensen, T. S. *J. Am. Chem. Soc.* **1994**, *116*, 3483−3493.

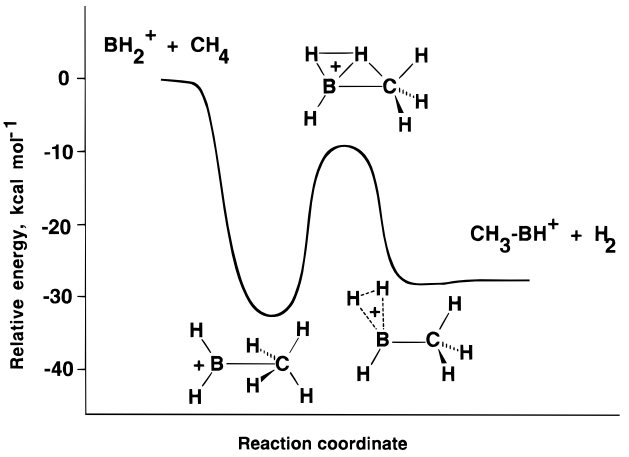

Figure 8. The calculated potential energy profile for the reaction of BH_2^+ with CH_4.

deep potential energy well, yet the reaction is rapid because of the high reaction exothermicity and an overall barrier that lies below the entrance channel. Therefore, the initial adduct does not live long enough to collide with helium atoms of the bath gas. Such collisions are necessary for removal of excess energy contained in the complex due to the exothermicity of its formation, and in their absence the reaction quickly proceeds further to products. For this reason no adduct formation was detected in the reaction of BH_2^+ with CD_4 under the conditions of our flowing afterglow experiments. However, formation of this species can be achieved by an indirect pathway, approaching it from lower energy reagents. We generated BH_4^+ ions in the reaction flow tube by adding H_2 to injected BH_2^+ (see above) and then added CD_4 downstream.[20] The desired adduct ion (*m*/*z* 33) results by a switching reaction in which CD_4 replaces H_2:

$$CD_4 + BH_4^+ \rightarrow CD_4{-}BH_2^+ + H_2$$

Because this reaction is exothermic by only 19 kcal mol^{-1} and because some of this exothermicity can be removed in the form of translational energy of the leaving hydrogen molecule, this reaction does not provide enough energy for $CD_4{-}BH_2^+$ to cross the central barrier (23 kcal mol^{-1}) to dissociation (Figure 8). Collisions with helium quickly stabilize the product of the reaction.

Reaction with Ethane. Ethane reacts even more rapidly than methane with BH_2^+ to form two products corresponding to loss of H_2 or CH_4, respectively:

$$CH_3{-}CH_3 + BH_2^+ \rightarrow \begin{cases} CH_3{-}CH_2{-}BH^+ + H_2 \\ CH_3{-}BH^+ + CH_4 \end{cases}$$

The first of these reactions is undoubtedly analogous to that with methane; this assumption is supported by our calculations which suggest structures homologous to those in Figure 7 and

(20) The reaction of BH_4^+ with CH_4 leads to $CH_4{-}BH_2^+$, which has the same *m*/*z* 29 as $HBOH^+$, the ion always present due to reaction of BH_2^+ with traces of water in helium buffer gas. The use of CD_4 gives the easily distinguishable adduct $CD_4{-}BH_2^+$ with *m*/*z* 33.

(21) Gioumousis, G.; Stevenson, D. P. *J. Chem. Phys.* **1958**, *29*, 294−299.

(22) Chesnavich, W. J.; Su, T.; Bowers, M. T. *J. Chem. Phys.* **1980**, *72*, 2641−2655.

(23) No suitable scaling factors are reported in the literature for systems with 3-center 2-electron bonds analogous to the systems studied. So we have not reported scaled zero-point energies. The authors thank a reviewer for pointing this out and for other valuable comments on the calculational part of this work.

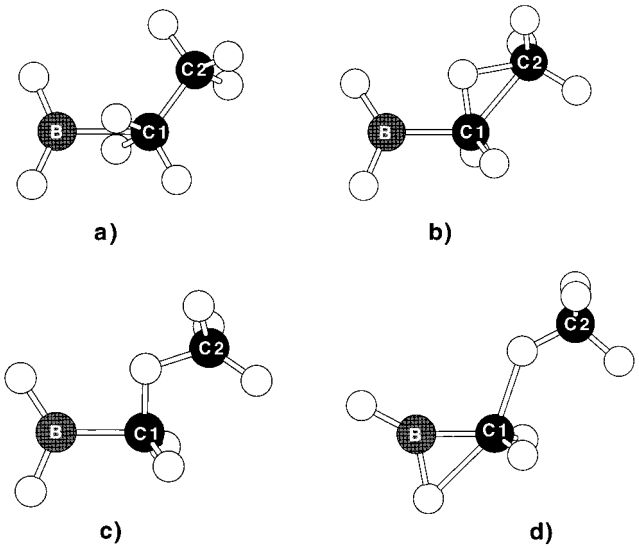

Figure 9. Molecular structures of species relevant to the reaction of BH_2^+ with C_2H_6 obtained from MP2(full)/6-311G(d,p) calculations.

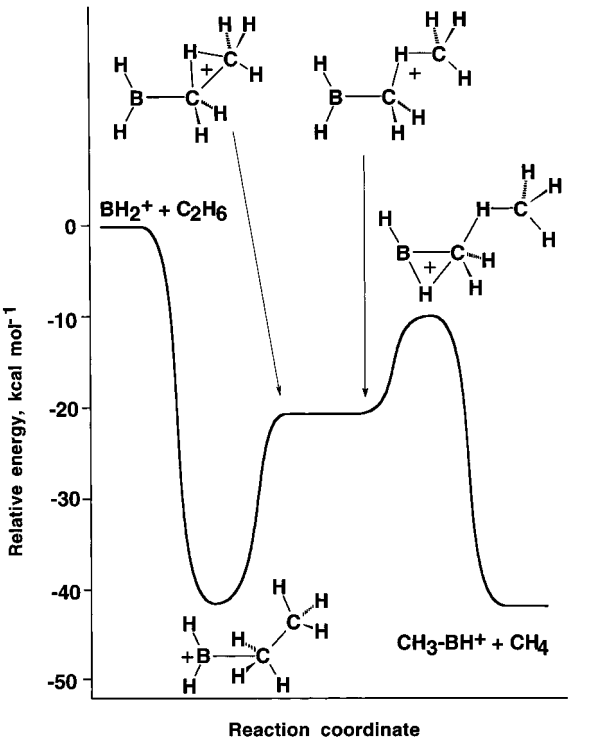

Figure 10. The calculated potential energy profile for the reaction of BH_2^+ with C_2H_6.

a reaction profile similar to that in Figure 8 for this channel. Experimental support of this parallelism is seen in the reaction of BD_2^+ with ethane resulting in exclusive loss of HD:

$$CH_3{-}CH_3 + BD_2^+ \rightarrow \begin{cases} CH_3{-}CH_2{-}BD^+ + HD \\ CH_2D{-}BD^+ + CH_4 \end{cases}$$

In the same reaction no deuterium atoms are incorporated into the CH_4 that is lost. Our calculations in conjunction with this experimental fact suggest that the channel leading to methane elimination involves the intermediacy of the structures presented in Figure 9 and has the energy profile presented in Figure 10. Formation of the adduct (structure **a** in Figure 9) is a common step for both reaction channels, but in contrast to reaction of BH_2^+ with methane there is an alternative of hydrogen shift

from C1 to C2 rather than from carbon to boron (compare Figure 9b to Figure 7b). Transition state **b** in Figure 9 leads to the complex of methane with a distorted $BH_2-CH_2^+$ structure (**c** in Figure 9). Direct dissociation of this complex is highly endothermic because relaxation of the $BH_2-CH_2^+$ fragment leads to an unfavorable perpendicular conformation of this unstable ion. Instead, the complex in Figure 9c undergoes a concerted isomerization−dissociation through the transition state represented by structure **d** in Figure 9, lowering the energetic barrier to products and resulting in stable CH_3BH^+.

Reactions with Other Reagents. Fast reactions of BH_2^+ with some other nucleophiles were also studied and are summarized in Table 1. All of these reactions follow the same general route discussed above for methane and ethane, that is, addition and elimination of a hydrogen molecule:

$$BH_2^+ + HR \rightarrow H-B-R^+ + H_2$$
$$R = OH, SH, NH_2, C_2H_3, C_2H$$

Excess water, ammonia, and hydrogen sulfide engage in a secondary reaction with these initial products and readily abstract a proton:

$$H-B-X-H^+ + H_2X \rightarrow H-B-X + H_3X^+$$
$$X = O, S, NH$$

The fact that formation of H_3O^+, H_3S^+, and NH_4^+ is indeed caused by secondary reactions, and not by competing direct proton abstraction from BH_2^+,

$$BH_2^+ + H_2X \rightarrow BH + H_3X^+$$

was established by measuring the ratio of the two products $HBXH^+$ and H_3X^+ at various flows of neutral reagents and different reaction times. These parameters influence the number of collisions each ion can experience with molecules of the neutral reagent. As the average number of reactive encounters for each ion approaches unity, the amount of the proton-transfer product decreases to zero and the primary addition−elimination product becomes dominant.

Reaction with ethylene yields the adduct as a minor by-product.

Conclusions

The title species, BH_2^+, undergoes a variety of reactions, many of which are similar to those of CH_3^+. In contrast to the methyl cation, the exothermicity of these reactions of BH_2^+ is moderate and their energy profiles are well defined, enabling a careful mechanistic study.

Along with a general route leading to $HB-R^+$ ($R = CH_3$, C_2H_5, OH, NH_2, etc.) some remarkable reactions were observed for BH_2^+, such as carbon−carbon bond cleavage in ethane and formation of adducts with one and two molecules of hydrogen.

Acknowledgment. C.H.D. and R.D. thank the National Science Foundation for support (CHE-9421756 for C.H.D. and CHE-9223037 for R.D.).

JA974005G